

Differential vulnerability of thalamic nuclei in multiple sclerosis

Simon Blyau^{1*}, Ismail Koubiyr^{2*}, Manojkumar Saranathan³, Pierrick Coupé⁴, Mathilde Deloire⁵, Julie Charré-Morin⁵, Aurore Saubusse⁵, Bei Zhang⁶, Brian Rutt⁷, Vincent Dousset^{1,2}, Bruno Brochet², Aurélie Ruet^{5,2}, Thomas Tourdias^{1,2}

¹ CHU de Bordeaux, Neuroimagerie diagnostique et thérapeutique, F-33000 Bordeaux, France

² Univ. Bordeaux, INSERM, Neurocentre Magendie, U1215, F-3300 Bordeaux, France

³ Department of Medical Imaging, University of Arizona, Tucson, AZ

⁴ Univ. Bordeaux, CNRS, Bordeaux INP, LABRI, UMR5800, F-33400 Talence, France

⁵ CHU de Bordeaux, Service de neurologie, F-33000 Bordeaux, France

⁶ Canon Medical Systems Europe, Zoetermeer, Netherlands

⁷ Department of Radiology, Stanford University, Stanford, CA

* Both authors contributed equally to this work.

Corresponding author:

Thomas Tourdias,

CHU de Bordeaux, Neuroimagerie diagnostique et thérapeutique, F-33000 Bordeaux, France

+33 (0)5 56 79 56 04

thomas.tourdias@chu-bordeaux.fr

Key words: MRI, thalamus, thalamic nuclei, segmentation, volumetry, differential vulnerability,

Abstract

Objectives: Investigating differential vulnerability of thalamic nuclei in MS.

Methods: In a secondary analysis of prospectively collected datasets, we pooled 136 patients with MS or clinically isolated syndrome and 71 healthy controls all scanned with conventional 3D-T1 and white-matter-nulled-MPRAGE (WMn-MPRAGE), and tested for cognitive performance. T1-based thalamic segmentation was compared with the reference WMn-MPRAGE method. Volumes of thalamic nuclei were compared according to clinical phenotypes and cognitive profile.

Results: T1- and WMn-MPRAGE provided comparable segmentations ($0.84 \pm 0.13 < \text{volume-similarity-index} < 0.95 \pm 0.03$). Medial and posterior thalamic groups were significantly more affected than anterior and lateral groups. Cognitive impairment related to volume loss of the anterior group.

Conclusion: Thalamic nuclei closest to the third ventricle are more affected, with cognitive consequences.

I. Introduction

Thalamic atrophy is a promising biomarker to quantify the overall neurodegeneration in MS because it results from both, focal white matter lesions transecting thalamocortical projections and causing in turn upstream/downstream thalamic degeneration, and also from direct grey matter (GM) attacks (1).

Cerebro-spinal-fluid (CSF)-mediated factors can drive subjacent damages in cortical GM (2). If such a CSF-mediated mechanism is also true for the thalamus, then thalamic nuclei closest to the third ventricle should exhibit a higher vulnerability; a hypothesis corroborated by confluent sub-ependymal demyelination in paraventricular thalamic nuclei on post-mortem brain (3), by more lesions adjacent to the third ventricle at ultra-high-field (1), and by a gradient of thalamic damage in pediatric MS (4).

However, due to challenges in accurately segmenting the thalamic nuclei, it is unclear whether regional volumetry could capture such differential neurodegenerative severity among thalamic nuclei and how this could relate to clinical performances.

We have previously optimized a white-matter-nulled version of MPRAGE (WMn-MPRAGE) at 7T to specifically enhance inter-thalamic nuclear contrast in close correlation with histological features (5). Leveraging manual segmentations from high resolution WMn-MPRAGE at 7T, we developed a multi-atlas segmentation method called THOMAS that automatically segment thalamus from WMn-MPRAGE input (6). Here, we adapted THOMAS to segment conventional T1 images, showed its validity against the reference WMn-MPRAGE-based method, and used this new tool to test whether differential thalamic vulnerability can be captured during the course of MS.

II. Methods

1. Population

We prospectively included 136 MS patients with various phenotypes (clinically isolated syndrome, CIS / early MS, n=71; relapsing-remitting, RRMS, n=51; primary-progressive, PPMS, n=14) and 71 healthy controls (HC), all explored with MRI and neuropsychological tests and Expanded Disability Status Scale (EDSS). Institutional review board approved the protocol and prior informed consent was obtained from all participants. More details in supplementary material.

2. MRI acquisitions and post-processing

All participants were scanned at 3T with conventional 3D-T1 and 99 of them (58 patients, 41 HC) were also explored with WMn-MPRAGE. We first compared segmentation from the original THOMAS algorithm using WMn-MPRAGE (6) with a modified version using conventional 3D-T1 and majority voting on participants where both sequences were acquired, using Dice similarity coefficient (DSC) and volume similarity index (VSI). Then, for all participants, eleven thalamic nuclei were segmented based on the conventional 3D-T1 method, then grouped into regions (anterior, lateral, medial, posterior), and volumetrically quantified by summing volumes from right and left hemispheres, normalizing by intra-cranial volume (ICV) and finally represented as Z-scores based on HC. More details in supplementary material.

3. Neuropsychological tests

Neuropsychological scores were converted to Z-scores based on the HC population. Patients were then classified as cognitively impaired (CI) for Z-score < -1.64 in at least two different cognitive domains, or otherwise cognitively preserved (CP). More details in supplementary material.

4. Statistical analyses

Demographic characteristics were compared between HC, CIS / early MS, RRMS and PPMS with Student t-test, Mann-Whitney or Chi-2 tests as appropriate. Z-scores of volumes were compared between thalamic groups with repeated measures ANOVA, and then, between clinical phenotypes as well as between CI and CP with MANCOVA. Correlations were tested with Spearman rank test. All tests were Bonferroni corrected except for Spearman correlations. IBM SPSS Statistics (v-25) and GraphPad (v-9.3) were used.

III. Results

1. Participant demographics

Table 1 summarizes the participant characteristics. As expected from these phenotypes representing different stages of neurodegenerative severity, we found a progressive increase of handicap and cognitive impairment from CIS / early MS to RRMS to PPMS.

2. T1-based segmentation efficiency

Supplementary Figure-1 shows comparison of segmentations using conventional T1 and WMn-MPRAGE as input images. The mean DSC for the whole thalamus and the 4 groups were between 0.65 ± 0.10 and 0.89 ± 0.02 and mean VSI between 0.84 ± 0.13 and 0.95 ± 0.03 indicating a fairly high degree of concordance.

3. Thalamic volumetric analyses

Whatever the stage of MS, the medial and posterior groups were always more affected than the anterior and lateral groups (Figure.1A-B and supplementary table 2 and Figure. 2). The comparison between phenotypes showed that the progressive volume loss of the whole thalamus was mainly driven by medial and posterior atrophy while the lateral group was relatively spared (Figure.1C). It can be noted that in patients with CIS / early MS , thalamic atrophy was only driven by volume loss from the medial group, while for RRMS patients with longer disease duration, medial and posterior groups were still the most important contributors but with additional contribution of anterior and lateral groups.

4. Associations between cognition, EDSS and thalamic volume loss

Supplementary tables 3 and 4 show the progressive worsening of cognitive performances from CIS / early MS to RRMS to PPMS and the correlations of thalamic groups with scores of individual cognitive domains. When it came to reaching threshold of clinical relevant cognitive impairment, only the anterior group was found significantly smaller in CI compared to CP after adjusting for age, sex, educational level and lesion load ($p<0.01$, Figure.1D). We found no correlations with EDSS.

IV. Discussion:

We have shown that differential thalamic vulnerability in MS is captured by regional atrophy and manifests itself from the early stages.

These data support the hypothesis of a 'surface-in' gradient of GM damage in MS, possibly through CSF-mediated toxic factors (7), because medial and posterior groups which are directly adjacent to the third ventricle were always more altered than anterior and mainly lateral groups which are further away from CSF. Damages secondary to transections of the thalamic projections are also likely to participate to more

widespread atrophy with longer disease duration. This gradient concept, originally developed after demonstration of 'pial-in' cortical gradient, is currently being mirrored to 'ependymal-in' for the thalamus (7). Neuropathology (3), quantitative MRI (4), and shape analysis (8) converge to this conclusion. However, whether volumetry of thalamic nuclei could be used as a relevant biomarker in this context is controversial because recent attempts with thalamic nuclei volumetry concluded to relatively homogeneous patterns of atrophy (9). Such discrepancy might be due to the inherent challenges in segmenting the thalamus on conventional T1 images that provide very low intra-thalamic contrast to guide the accurate identification of the boundaries (5,6). By maximizing intra-thalamic contrast with WMn-MPRAGE, we previously showed better performances than the Freesurfer method (6) while being closely correlated with the histological Morel atlas (5). Here, we implemented a variant of the original THOMAS algorithm that is a majority-voting based multi-atlas segmentation with conventional T1 input. We obtained DSC and VSI close enough to the reference WMn-MPRAGE to rely on these segmentations.

In terms of clinical impact, while medial and posterior thalamus were correlated with cognitive performances (supplementary table 4), their early atrophy might be balanced by compensatory mechanisms. Progression of atrophy to the anterior group might overwhelm compensation and induce clinically significant impairment in line with data pointing toward integrity of anterior thalamic radiations as a strong predictor of CI (8,10,11).

Limitations include the cross-sectional nature of the study and the low range of EDSS severity that can contribute to difficulty in finding correlations with this score. We also acknowledge that we pooled control participants associated with each disease phenotype into a single group, which ultimately led to some variability in this group. Finally, different definitions of thalamic nuclei and groups can be found but we would expect consistent finding even with alternative definitions.

Overall, we provided a method for thalamic nuclei volumetry that highlighted candidate biomarkers to capture *in vivo* the surface-in thalamic gradient with possible future impact for prognosis and monitoring.

Funding

This work was supported by was supported by the TRAIL (Translational Research and Advanced Imaging Laboratory), laboratory of excellence (ANR-10-LABX-57). The SCICOG study was also supported by a grant from TEVA and ARSEP (Fondation pour l'Aide à la Recherche sur la Sclérose En Plaques). The SOCOG and MICROSEP studies were supported by a grant from the Bordeaux University Hospital. The PROCOG study was supported by a grant from Roche. The AUBACOG study was supported by a grant from Genzyme. This work has been performed with the help of the OFSEP (Observatoire Français de la Sclérose En Plaques), which is supported by a grant provided by the French State and handled by the "Agence Nationale de la Recherche", within the framework of the "Investments for the Future" program, under the reference no. ANR-10-COHO-002.

Conflict of interest

SB: Nothing to declare

IK: Received research grants from LabEx TRAIL (Translational Research and Advanced Imaging Laboratory) and ARSEP (Fondation pour l'Aide à la Recherche sur la Sclérose En Plaques). He received speakers' honoraria from Celgene.

MS: Nothing to declare

PC: Nothing to declare

MD: Nothing to declare

JCM: Nothing to declare

AS: Nothing to declare

BZ: employee of Canon Medical

BR: Nothing to declare

VD: Member of the medical advisory board of Canon Medical.

BB: reports grants from the French Ministry of Health during the conduct of the study; personal fees and non-financial support from Biogen-idec, grants from Merck-Serono, personal fees and non-financial support from Novartis, personal fees and non-financial support from Genzyme, grants, personal fees and non-financial support from TEVA, grants and non-financial support from Bayer, outside the submitted work.

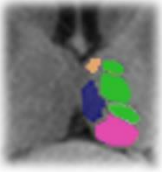
AR: reports grants from TEVA, during the conduct of the study; personal fees and non-financial support from Novartis, personal fees and non-financial support from Biogen, grants, personal fees and non-financial support from TEVA, grants and non-financial support from Roche, grants and non-financial support from Merck, grants and non-financial support from Genzyme, non-financial support from Medday, grants from Bayer, outside the submitted work.

TT: Received support from Roche and Canon Medical. Received recent grant supports from Idex Bordeaux, Bordeaux University Hospital, labEx BRAIN and the national program for clinical research (PHRC).

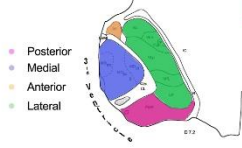
References

1. Ontaneda D, Raza PC, Mahajan KR, Arnold DL, Dwyer MG, Gauthier SA, et al. Deep grey matter injury in multiple sclerosis: a NAIMS consensus statement. *Brain*. 2021 Aug 17;144(7):1974–84.
2. Howell OW, Reeves CA, Nicholas R, Carassiti D, Radotra B, Gentleman SM, et al. Meningeal inflammation is widespread and linked to cortical pathology in multiple sclerosis. *Brain*. 2011 Sep;134(9):2755–71.
3. Gilmore CP, Donaldson I, Bo L, Owens T, Lowe J, Evangelou N. Regional variations in the extent and pattern of grey matter demyelination in multiple sclerosis: a comparison between the cerebral cortex, cerebellar cortex, deep grey matter nuclei and the spinal cord. *Journal of Neurology, Neurosurgery & Psychiatry*. 2009 Feb 1;80(2):182–7.
4. De Meo E, Storelli L, Moiola L, Ghezzi A, Veggiotti P, Filippi M, et al. *In vivo* gradients of thalamic damage in paediatric multiple sclerosis: a window into pathology. *Brain*. 2021 Feb 12;144(1):186–97.
5. Tourdias T, Saranathan M, Levesque IR, Su J, Rutt BK. Visualization of intra-thalamic nuclei with optimized white-matter-nulled MPRAGE at 7T. *NeuroImage*. 2014 Jan;84:534–45.
6. Su JH, Thomas FT, Kasoff WS, Tourdias T, Choi EY, Rutt BK. Thalamus Optimized Multi Atlas Segmentation (THOMAS): fast, fully automated segmentation of thalamic nuclei from structural MRI. *NeuroImage*. 2019 Jul;194:272–82.
7. Pardini M, Brown JWL, Magliozzi R, Reynolds R, Chard DT. Surface-in pathology in multiple sclerosis: a new view on pathogenesis? *Brain* 2021 Jul; 144(6):1646-1654
8. Bergsland N, Zivadinov R, Dwyer MG, Weinstock-Guttman B, Benedict RH. Localized atrophy of the thalamus and slowed cognitive processing speed in MS patients. *Mult Scler*. 2016 Sep;22(10):1327–36.
9. Bergsland N, Benedict RHB, Dwyer MG, Fuchs TA, Jakimovski D, Schweser F, et al. Thalamic Nuclei Volumes and Their Relationships to Neuroperformance in Multiple Sclerosis: A Cross-Sectional Structural MRI Study. *J Magn Reson Imaging*. 2021 Mar;53(3):731–9.
10. Eijlers AJC, van Geest Q, Dekker I, Steenwijk MD, Meijer KA, Hulst HE, et al. Predicting cognitive decline in multiple sclerosis: a 5-year follow-up study. *Brain* 2018 Jul; 141(9):2605-2618
11. Aggleton JP, O'Mara SM. The anterior thalamic nuclei: core components of a tripartite episodic memory system. *Nat Rev Neurosci*. 2022 Apr

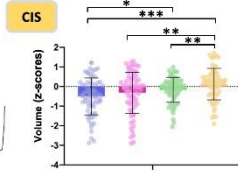
A1



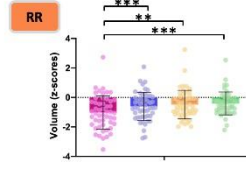
2



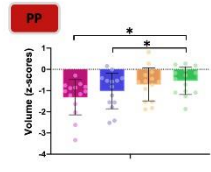
B1



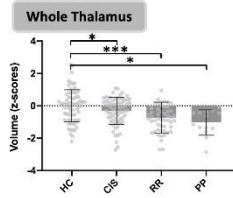
2



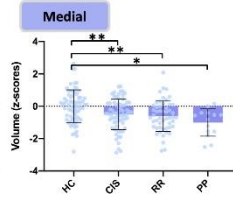
3



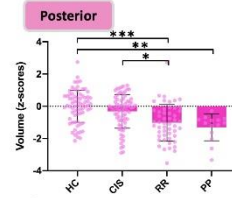
C1



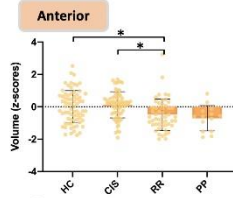
2



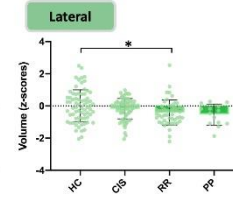
3



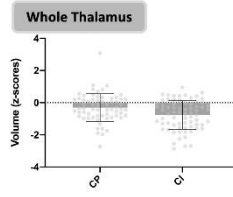
4



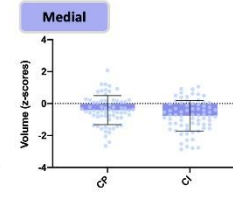
5



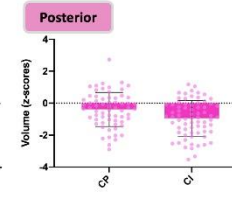
D1



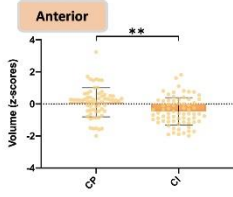
2



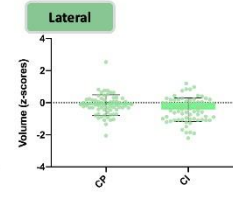
3



4



5



Groups	HC n=71	MS n=136	CIS n=71	RR n=51	PP n=14
Age (years), mean (SD)	39.86 ± 8.85	40.03 ± 11.08	36.71 ± 10.90	41.37 ± 9.61	51.95 ± 7.66***
p value		0.99	0.18	0.99	<0.001
Gender (female), n (%)	47 (66%)	101 (74%)	56 (79%)	36 (71%)	9 (64%)
p value		0.89	0.36	0.99	0.99
Education (years), mean (SD)	14.21 ± 2.54	13.51 ± 2.67	13.62 ± 2.67	13.67 ± 2.78	12.31 ± 2.06 *
p value		0.24	0.58	0.99	0.040
Baccalaureate level (yes), n (%)	51 (77%)	96 (71%)	51(72%)	39 (77%)	6 (43%)
p value		0.99	0.99	0.99	0.052
Disease duration (years), mean (SD)	-	4.4 ± 6.1	0.4 ± 0.1	9.7 ± 6.7§§§	5.3 ± 2.4§§§
p value		-	-	<0.001	<0.001
EDSS (score), mean (SD)	-	1.50 ± 1.40	1.25 ± 1.11	1.50 ± 1.19	3.74 ± 1.45§§§
p value		-	-	0.99	<0.001
Lesion load † (mL), mean (SD)	-	6111 ± 10972	4040 ± 9312	8060 ± 9571§§§	9643 ± 19312§
p value		-	-	<0.001	0.0360
CP , n (%)	-	80 (59%)	45 (63%)	30 (59%)	5 (36%)
CI , n (%)	-	56 (41%)	26 (37%)	21 (41%)	9 (64%)
p value		-	-	0.61	0.06

Table 1: Characteristics of participants.

CI: cognitively impaired, CIS: clinically isolated syndrome, CP: cognitively preserved, EDSS: expanded disability status scale, HC: healthy control, MS: multiple sclerosis, RR: relapsing remitting, PP: primary progressive, SD: standard deviation.

† White matter lesion load was quantified from 3D-FLAIR (<http://volbrain.upv.es>).

* and *** are for $p < 0.05$ and $p < 0.001$ for patients versus controls (Student t-test, Mann-Whitney test or Chi-2 test as appropriate), § and §§§ are for $p < 0.05$ and $p < 0.001$ for patients versus CIS (Mann-Whitney test). Bonferroni corrections accounted for the overall number of pairwise comparisons. Missing data, in the HC group, for n=5 for ‘education’ and ‘baccalaureate level’; in the MS group, for n=1 for ‘disease duration’, ‘EDSS’ and ‘education’.

Differential vulnerability of thalamic nuclei in multiple sclerosis

Supplementary materials

I. Supplementary methods

5. Population

The participants were recruited as part of 5 prospective studies named MICROSEP, SCICOG, SOCOG, AUBACOG, PROCOG (clinical trial registration numbers NCT03692975, NCT01865357, NCT02290587, NCT03768648, NCT03455582 respectively), all aiming at studying the underlying substrate of cognitive impairment at different stages of multiple sclerosis (MS). Patients within the “CIS / early MS” group came from MICROSEP and SCICOG studies and were included within the 6 months following a first clinical episode compatible with a demyelinating inflammatory episode potentially suggestive of MS whatever the mode of presentation. They should also present at least two clinically silent lesions on their T2-weighted brain or spinal MRI scan with a size of least 3 mm, at least one of which being cerebral, ovoid, or periventricular. They were classified early MS if they met the 2017 Mc-Donald criteria (1) for dissemination in time and space (n=55), and CIS otherwise (n=16 among which 6 met criteria for dissemination in space). The other patients were relapsing remitting (RR; n=51) or primary progressive (PP; n=14) MS according to the 2017 Mc-Donald criteria (1). Exclusion criteria included age below 18 years, inability to undergo MRI, inability to have MRI acquisitions distant of, at least, one month from corticoid treatment and acute attack, history of other neurological or psychiatric disorders and severe depression (Beck Depression Inventory >27). Seventy-three healthy controls (HC) recruited as part of the above-mentioned prospective studies were pooled into a single control group.

From the initial cohort of 137 patients and 73 HC, one patient was excluded because of many consecutive attacks close to MRI acquisition and two healthy controls were also excluded because of their medical history, leaving 136 patients and 71 HC for the analysis.

6. MRI acquisitions and post-processing

Acquisitions

All the MRI acquisitions were acquired on 3T MRI systems (Achieva TX system, Philips Healthcare; Discovery MR 750w, GE Healthcare; Vantage Galan ZGO, Canon Medical) at least one month apart from corticoid treatment and acute clinical attack.

All the imaging protocols included conventional 3D-T1 weighted images and 3D or 2D-FLAIR for the 207 participants. This complete dataset was used for the primary analysis. After an update of our imaging protocols, white-matter-nulled MPRAGE (WMn-MPRAGE) was added following previously published recommendations to enhance intra-thalamic contrast at 3T (2,3). This sequence was available for a subset of 58 MS patients and 41 HC and we used this second dataset to compare the thalamic segmentations originating from WMn-MPRAGE and conventional 3D-T1.

Supplementary Table 1 summarizes the acquisition parameters.

	T1-wi		FLAIR			WMn MP-RAGE		
	IR-FSPGR	CSFn-MPRAGE						
Number of subjects MS (n) / HC (n)	77/29	59/42	59/42	20/15	57/14	3/0	17/3	38/38
2D/3D Plane	3D/axial	3D/Sagittal	3D-Sagittal 1.03 x 1.03 x 1	3D-Sagittal	2D/Axial 0.65 x 0.65 x 3.3	3D/Coronal	3D/Coronal	3D/Axial
Voxel size (mm³)	1 x 1 x 1	1 x 1 x 1	1	1 x 1 x 0.7		1.5 x 1.5 x 1	1 x 1 x 1	1 x 1 x 1
Matrix (voxel)	256 x 256 x 176	224 x 224 x 180	224 x 224 x 180	256 x 256 x 272	230 x 230 x 46	128 x 128 x 220	180 x 190 x 176	190 x 176
TR (ms)	8.2	6.3	7000	7200	11000	8.5	8.5	7.8
TE (ms)	3.5	2.8	445.5	136.3	140	3.9	3.9	3.6
TI (ms)	982	950	2100	1939	2800	500	500	570
α (°)	7	9	90	90	90	7	7	7

Supplementary Table 1: Acquisition parameters of the conventional 3D-T1 images, FLAIR and WMn-MPRAGE.

CSFn: cerebrospinal fluid nulled; FLAIR: fluid attenuated inversion recuperation; HC: healthy controls; IR-FSPGR: inversion recovery fast spoiled gradient-echo with magnetization prepared; MPRAGE: magnetization preparation rapid acquisition gradient echo, WMn: white-matter-nulled.

Post-processing

The WMn-MPRAGE images were used to segment the thalamus by using the multi-atlas method that we called THOMAS (4). This method leverages from a library of 20 priors high resolution and high contrast 7Tesla WMn-MPRAGE images (4) that have been manually segmented in close correlation with the histological Morel atlas thanks to the inherent contrast that is generated from such as sequence (3).

For the 3D-T1 weighted images, we implemented a modification of the original THOMAS method that we have used recently (5). The method is identical to the original THOMAS but uses T1 as image input that is registered to the template of priors using the nonlinear symmetric image normalization (SyN) algorithm implemented in ANTs (6). Each anatomical prior was also registered to the template image and these were available *a priori*. A single composite transformation to warp each anatomical prior to each subject's T1-weighted image was then generated by combining the prior to template warp with the template to subject warp. This composite transformation was applied to all thalamic nuclei labels from each of the anatomical priors, to produce sets of thalamic nuclei labels aligned with each subject's image. Finally, the sets of candidate labels (one from each prior in the library) were fused to create a single set of labels for the target T1 image using majority voting (7) as implemented in ANTs instead of joint label fusion that was used in the original THOMAS method (4).

Both methods produced 11 thalamic nuclei that were combined into 4 main groups based on anatomical and functional considerations (8) following the definitions found in Morel atlas :

- anterior group: anteroventral (AV)
- lateral group: ventral posterolateral (VPL), ventral lateral anterior (VLa), ventral lateral posterior (VLp), and ventral anterior (VA)
- medial group: mediodorsal (MD), centromedian (CM), and habenula (Hb) (part of the epithalamus but comprised in the paraventricular complex and located at the infero-postero-medial part of the medial group and so very close to the 3rd ventricle)
- posterior group: pulvinar (Pul), medial geniculate nucleus (MGN), and lateral geniculate nucleus (LGN)

In order to compare the T1-based segmentation method described above with the direct segmentation from WMn-MPRAGE, we used Dice similarity coefficient (DSC) and volume similarity index (VSI). DSC quantifies the overlap of segmentations from two different methods with Dice 1 corresponding to perfect overlap. VSI equals one minus the absolute value of the difference of the segmentation volumes over the sum of the two volumes, with VSI of 1 corresponding to volumes being identical.

$$Dice = 2 \times \frac{|X \cap Y|}{|X| + |Y|}$$

$$VSI = 1 - \frac{abs(|X| - |Y|)}{|X| + |Y|}$$

where X and Y refer to the 2 segmentation masks and |X| and |Y| refer to the number of voxels in X and Y, respectively.

For the volumetric analysis of the whole cohort, T1-based volumes of right and left sides were summed and divided by the volume of the intra-cranial cavity extracted through AssemblyNet software (9) to compensate for inter-subject variability. Furthermore, to be able to compare accurately groups of thalamic nuclei whose sizes are different, Z-scores were calculated for all the normalized volumes (in percentage of ICV) using HC values. Overall, such Z-score of normalized volumes compensated both inter-subject and inter-nucleus variability in size.

7. Neuropsychological tests

Neuropsychological tests were administered by two experienced neuropsychologists specialized in MS. Participants were evaluated with a battery of neuropsychological tests at the time of MRI, which was at least one month after corticoid treatment and acute attack.

Specific tests were used for each domain. Information processing speed was evaluated by the Computerized Speed Cognitive Test (CSCT; sum). Verbal memory was evaluated by the California Verbal Learning Test list A (CVLTA; sum, long-term retrieval LTR) or the Selective Reminding Test (SRT; long-term storage LTS, consistent long-term retrieval CLTR, delay recall DR). Visual memory was evaluated by the Brief Visuospatial Memory Test-Revised (BVMTR; sum, delay recall DR). Working memory was evaluated by the Paced-Auditory Serial Addition Test-3s (PASAT; correct answer CA). Executive functions were evaluated by the forward and backward digit span test considering the executive component from the backward digit span. Attention was evaluated by visual scanning with target that is part of the Test of Attentional Performance (TAP; time, omitted answers).

Five HC did not take the neuropsychological tests. Among the MS group, one CIS / early MS patient was not able to complete the BVMT-R test. Two RRMS patients and

two PPMS patients were not able to complete the PASAT. One CIS / early MS patient and one PPMS patient were not able to achieve the TAP.

Performance of patients were compared with those of HC by computing Z-scores for each test.

$$Z - Score = \frac{Patient\ Score - Mean\ of\ HC}{Standard\ Deviation\ of\ HC}$$

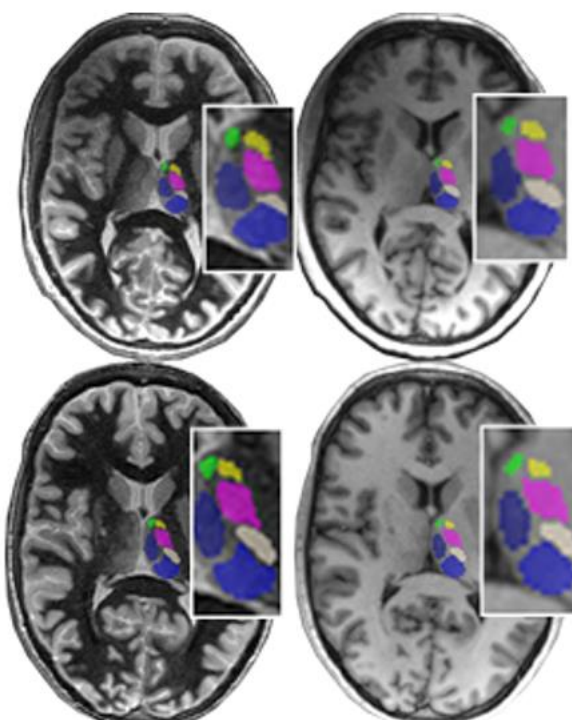
Therefore, lower Z-score indicates lower performance and a patient was considered cognitively impaired if he/she showed Z-score <-1.64 (corresponding to a performance below the lower fifth percentile) in at least two different cognitive domains according to agreed-upon threshold (10,11). This method is commonly used in neuropsychological studies in MS (10–13).

II. Supplementary results

5. T1-based segmentation efficiency

Means DSC and VSI are presented for the whole thalamus, groups of thalamic nuclei and individual thalamic nuclei and an example from one MS patient and from one HC are presented in the supplementary figure 1.

	Dice	VSI
	Mean SD	Mean SD
Thalamus	0.89 ± 0.02	0.95 ± 0.03
Medial	0.79 ± 0.05	0.84 ± 0.12
Posterior	0.77 ± 0.05	0.87 ± 0.08
Lateral	0.75 ± 0.05	0.94 ± 0.04
Anterior	0.65 ± 0.10	0.84 ± 0.13
MD	0.80 ± 0.06	0.82 ± 0.13
Pul	0.79 ± 0.05	0.88 ± 0.07
VLp	0.76 ± 0.06	0.92 ± 0.05
VA	0.71 ± 0.07	0.88 ± 0.07
AV	0.65 ± 0.10	0.84 ± 0.13
VPL	0.62 ± 0.11	0.88 ± 0.08
LGN	0.59 ± 0.08	0.64 ± 0.17
MGN	0.59 ± 0.11	0.74 ± 0.19
CM	0.58 ± 0.14	0.89 ± 0.08
VLa	0.54 ± 0.09	0.83 ± 0.13
Hb	0.53 ± 0.09	0.52 ± 0.28



Supplementary Figure 1: DSC and VSI for the whole thalami, the groups and the individual nuclei computed from the T1- and WMn-MPARGe-based segmentations (left part of the figure).

Representations of thalamic segmentations (right part of the figure) with THOMAS segmentation over WMn acquisition (left part) and the modified version of THOMAS over conventional 3D-T1 acquisition (right part) for a healthy control (upper part) and a MS patient (bottom part).

SD: standard deviation, VSI: volume similarity index, Pul: pulvinar, VLp: ventral lateral posterior, MD: mediodorsal, VPL: ventral posterolateral, VA: ventral anterior, AV: anteroventral, CM: centromedian, LGN: lateral geniculate nucleus, VLa: ventral lateral anterior, MGN: medial geniculate nucleus, Hb: habenula.

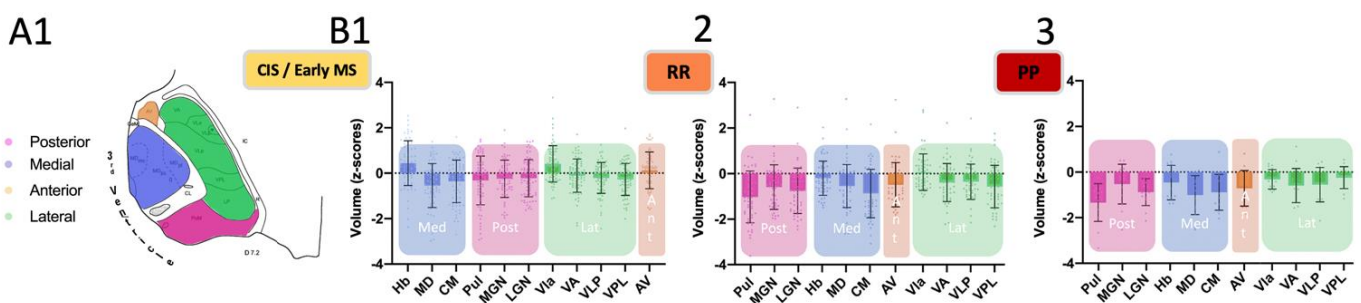
6. Thalamic volumetric analyses

In addition to Z-score, the absolute volumetric values of the whole thalamus and the thalamic groups were reported in supplementary table 2. Right and left side volumes were summed for each structure.

Groups	HC n=71	MS n=136	CIS / early MS n=71	RR n=51	PP n=14
Thalamus total , mean, SD (mm ³)	11026 ± 1297	9721 ± 1562	9897 ± 1573	9623 ± 1536	9181 ± 1556
Medial , mean, SD (mm ³)	1496 ± 213	1271 ± 270	1277 ± 274	1289 ± 269	1180 ± 247
Anterior , mean, SD (mm ³)	247 ± 43	224 ± 46	237 ± 43	212 ± 48	203 ± 41
Posterior , mean, SD (mm ³)	2938 ± 433	2494 ± 544	2614 ± 553	2390 ± 512	2257 ± 478
Lateral , mean, SD (mm ³)	3173 ± 480	2936 ± 431	2988 ± 411	2916 ± 447	2743 ± 443

Supplementary Table 2: Absolute values of volumes (means and SD) for the whole thalamus and the nuclear groups of controls and patients. Both sides of the structures were summed. HC: healthy control, MS: multiple sclerosis, CIS: clinically isolated syndrome, RR: relapsing remitting, PP: primary progressive, SD: standard deviation.

In complement to the 4 main groups, individual nuclei within each group were also represented in supplementary figure 2. It reinforces the data showing that individual nuclei within a given group behaved pretty similarly to the mean value within the group (except the habenula which is very small and possibly inaccurately segmented according to supplementary figure 1).



Supplementary Figure 2:

Individual nuclei are gathered into 4 groups (anterior, lateral, medial, and posterior) as illustrated on the corresponding Morel plate (A1). B1-3 shows the volumetric Z-scores of the individual thalamic nuclei within each group. CIS: clinically isolated syndrome, MS: multiple sclerosis, RR: relapsing remitting, PP: primary progressive, Med : medial, Post : posterior, Lat : lateral, Ant :anterior, Hb: habenula, MD: mediodorsal, CM: centromedian, Pul: pulvinar, MGN: medial geniculate nucleus, LGN: lateral geniculate nucleus, VLa: ventral lateral anterior, VA: ventral anterior, VLp: ventral lateral posterior, VPL: ventral posterolateral), AV: anteroventral).

7. Cognitive results

Mean Z-scores for each cognitive domain are presented in supplementary table 3 according to the MS phenotype. Cognitive performances were already significantly decreased in CIS / early MS for almost all the domains and progressively worsened in RRMS and PPMS groups.

Verbal memory was only altered for PP patients. Working memory was not altered for the PPMS group which may be a consequence of the small number of subjects that caused Z-score dispersion even if their mean Z-score was lower than CIS / early MS and RRMS.

Executive functions were not altered which is consistent with recent data on staging of cognitive deficits (14) and which could also be linked to the fact that classical tests exploring this domain may not be sensitive to discriminate well HC from MS patients (15).

Cognitive Domains	MS n=136	CIS / early MS n=71	RRMS n=51	PPMS n=14
Information processing speed	-0.83 ± 1.40***	-0.72 ± 1.30**	-0.67 ± 1.32*	-2.00 ± 1.71**
p value	<0.001	0.007	0.018	0.005
Verbal memory	-0.48 ± 1.38	-0.30 ± 1.32	-0.59 ± 1.47	-1.02 ± 1.25**
p value	0.187	1.829	0.376	0.007
Visual memory	-0.76 ± 1.48**	-0.78 ± 1.49**	-0.44 ± 1.08*	-1.79 ± 2.14**
p value	0.0001	0.0038	0.0275	0.0002
Working memory	-0.73 ± 1.34***	-0.70 ± 1.25**	-0.59 ± 1.27*	-1.57 ± 2.00
p value	<0.001	0.002	0.037	0.074
Executive functions	-0.18 ± 0.90	-0.24 ± 0.71	-0.03 ± 1.14	-0.48 ± 0.73
p value	1.5970	1.2335	5.8373	0.6005
Attention	-0.67 ± 1.23***	-0.53 ± 0.86***	-0.58 ± 1.00**	-1.79 ± 2.64**
p value	<0.001	<0.001	0.005	0.003

Supplementary Table 3: Z-scores for the cognitive performances of the different phenotypes of MS patients. Values are mean ± standard deviation. One CIS /early MS patient was not able to complete the BVMTR test. Two RRMS patients and two PPMS patients were not able to complete the PASAT. One CIS /early MS patient and one PPMS patient were not able to achieve the TAP.

MS: multiple sclerosis, HC: healthy control, CIS: clinically isolated syndrome, RR: relapsing remitting, PP: primary progressive, CI: cognitively impaired, CP: cognitively preserved, N: number, SD: standard deviation. * $p < 0.05$, ** $p < 0.01$, *** $p < 0.001$ for Mann Whitney or Student t-test comparisons with HC as appropriate with Bonferroni

Correlation analyses between thalamic volumes and each cognitive scores are presented in supplementary table 4. It shows that information processing speed reflected global dysfunction (12) and that lateral group, which is mainly involved in motor functions (8), was not involved in most cognitive functions. It also shows associations of the anterior group with memory functions in line with the core role of this group in memory system (16). Medial and posterior groups were also correlated with memory functions which is expected regarding the role of the medial group in recognition memory and the role of the posterior group in language and therefore in verbal memorization (8). Executive functions were correlated with medial and posterior atrophy. Medial group is known to be implicated in executive functions and bilateral infarction of medial nuclei can lead to frontal syndrome (8). Attention was correlated with posterior and anterior atrophy in line with involvement of the posterior group in visual attention (17) and of the anterior group in global attention (18).

		Information speed processing	Verbal memory	Visual memory	Working memory	Executive functions	Attention
Thalamus	corr coef	0.381	0.256	0.130	0.082	0.220	0.176
	p-value	<0.001	0.003	0.132	0.353	0.010	0.042
Medial	corr coef	0.332	0.306	0.110	0.101	0.292	0.124
	p-value	<0.001	<0.001	0.205	0.250	0.001	0.153
Anterior	corr coef	0.299	0.246	0.219	0.100	0.154	0.182
	p-value	<0.001	0.004	0.011	0.255	0.074	0.035
Posterior	corr coef	0.399	0.282	0.111	0.114	0.211	0.223
	p-value	<0.001	0.001	0.200	0.193	0.014	0.010
Lateral	corr coef	0.220	0.071	0.118	0.002	0.148	0.052
	p-value	0.010	0.410	0.172	0.979	0.086	0.554

Supplementary Table 4: Bivariate correlations between cognitive Z-scores, the whole thalamus and the nuclear groups. One patient was not able to complete visual memory tests, five were not able to complete working memory tests and two were not able to complete attention tests. Significant correlations are in blue. Corr coef: correlation coefficient.

References

1. Thompson AJ, Banwell BL, Barkhof F, Carroll WM, Coetzee T, Comi G, et al. Diagnosis of multiple sclerosis: 2017 revisions of the McDonald criteria. *Lancet Neurol*. 2018 Feb;17(2):162–73.
2. Saranathan M, Tourdias T, Bayram E, Ghanouni P, Rutt BK. Optimization of white-matter-nulled magnetization prepared rapid gradient echo (MP-RAGE) imaging: Optimization of White-Matter-Nulled MP-RAGE Imaging. *Magn Reson Med*. 2015 May;73(5):1786–94.
3. Tourdias T, Saranathan M, Levesque IR, Su J, Rutt BK. Visualization of intrathalamic nuclei with optimized white-matter-nulled MPRAGE at 7T. *NeuroImage*. 2014 Jan;84:534–45.
4. Su JH, Thomas FT, Kasoff WS, Tourdias T, Choi EY, Rutt BK. Thalamus Optimized Multi Atlas Segmentation (THOMAS): fast, fully automated segmentation of thalamic nuclei from structural MRI. *NeuroImage*. 2019 Jul;194:272–82.
5. the Alzheimer's Disease Neuroimaging Initiative, Bernstein AS, Rapcsak SZ, Hornberger M, Saranathan M. Structural Changes in Thalamic Nuclei Across Prodromal and Clinical Alzheimer's Disease. *J Alzheimers Dis*. 2021 Jun 29;82(1):361–71.
6. Avants BB, Tustison NJ, Song G, Cook PA, Klein A, Gee JC. A reproducible evaluation of ANTs similarity metric performance in brain image registration. *NeuroImage*. 2011 Feb;54(3):2033–44.
7. Rohlfing T, Brandt R, Menzel R, Maurer CR. Evaluation of atlas selection strategies for atlas-based image segmentation with application to confocal microscopy images of bee brains. *NeuroImage*. 2004 Apr;21(4):1428–42.
8. Herrero MT, Barcia C, Navarro J. Functional anatomy of thalamus and basal ganglia. *Childs Nerv Syst*. 2002 Aug 1;18(8):386–404.
9. Coupé P, Mansencal B, Clément M, Giraud R, Denis de Senneville B, Ta VT, et al. AssemblyNet: A large ensemble of CNNs for 3D whole brain MRI segmentation. *NeuroImage*. 2020 Oct;219:117026.
10. Ruet A, Deloire M, Hamel D, Ouallet JC, Petry K, Brochet B. Cognitive impairment, health-related quality of life and vocational status at early stages of multiple sclerosis: a 7-year longitudinal study. *J Neurol*. 2013 Mar;260(3):776–84.
11. Amato MP, Morra VB, Falautano M, Ghezzi A, Goretti B, Patti F, et al. Cognitive assessment in multiple sclerosis—an Italian consensus. *Neurol Sci*. 2018 Aug;39(8):1317–24.
12. Benedict RHB, Amato MP, DeLuca J, Geurts JJG. Cognitive impairment in multiple sclerosis: clinical management, MRI, and therapeutic avenues. *Lancet Neurol*. 2020 Oct;19(10):860–71.

13. Meca-Lallana V, Gascón-Giménez F, Ginestal-López RC, Higuera Y, Téllez-Lara N, Carreres-Polo J, et al. Cognitive impairment in multiple sclerosis: diagnosis and monitoring. *Neurol Sci.* 2021 Dec;42(12):5183–93.
14. Wojcik C, Fuchs TA, Tran H, Dwyer MG, Jakimovski D, Unverdi M, et al. Staging and stratifying cognitive dysfunction in multiple sclerosis. *Mult Scler J.* 2021 May; 28(3):463-471.
15. Realdon O, Serino S, Savazzi F, Rossetto F, Cipresso P, Parsons TD, et al. An ecological measure to screen executive functioning in MS: the Picture Interpretation Test (PIT) 360°. *Sci Rep.* 2019 Dec;9(1):5690.
16. Aggleton JP, O'Mara SM. The anterior thalamic nuclei: core components of a tripartite episodic memory system. *Nat Rev Neurosci.* 2022 Apr
17. Rees G. Visual Attention: The Thalamus at the Centre? *Curr Biol.* 2009 Mar;19(5):R213–4.
18. Leszczyński M, Staudigl T. Memory-guided attention in the anterior thalamus. *Neurosci Biobehav Rev.* 2016 Jul;66:163–5.